

Photoinduced spin crossover in Fe-picolylamine complex: A farinfrared study on single crystals

H. Okamura,^{*} M. Matsubara, and T. Nanba

*Graduate School of Science and Technology,
Kobe University, Kobe 657-8501, Japan.*

T. Tayagaki,[†] S. Mouri, and K. Tanaka

*Department of Physics, Graduate School of Science,
Kyoto University, Kyoto 606-8502, Japan.*

Y. Ikemoto, T. Moriwaki, and H. Kimura

Japan Synchrotron Radiation Research Institute and SPring-8, Sayo 679-5198, Japan.

G. Juhász[‡]

Department of Chemistry, Kyushu University, Fukuoka 812-8581, Japan.

(Dated: August 15, 2018)

Abstract

Farinfrared spectroscopy has been performed on $[\text{Fe}(\text{2-picolylamine})_3]\text{Cl}_2\text{EtOH}$ (Fe-pic) single crystals, to probe changes in the molecular vibrations upon the photoinduced and temperature-induced spin crossovers. Synchrotron radiation has been used as the farinfrared source to overcome the strong absorption and the small sizes of the samples. Absorption lines due to FeN_6 cluster vibrations, observed below 400 cm^{-1} , show strong intensity variations upon the crossover due to the deformation of FeN_6 between high-spin and low-spin states. However, they remain almost unchanged between the photo- and temperature-induced high-spin states. This is in sharp contrast to the lines at $500\text{--}700\text{ cm}^{-1}$ due to intramolecular vibrations of the picolylamine ligands, which show marked variations between the two high-spin states. It is concluded that the most important microscopic difference between the two high-spin states arises from the ligands, which is likely to reflect different states of intermolecular bonding between them.

PACS numbers: 75.30.Wx, 78.30.-j

[Fe(2-pic)₃]Cl₂EtOH (2-pic: 2-picolyamine or 2-aminomethyl pyridine, EtOH: ethanol), referred to as the Fe-pic, is one of the Fe(II)-based complexes which have recently attracted much interest for exhibiting a photoinduced spin crossover.^{1,2,3} As sketched in Fig. 1(a), an Fe²⁺ ion in Fe-pic is located in a nearly octahedral crystal field created by the three 2-pic ligands. Depending on the magnitude of the crystal field splitting, Fe²⁺ takes either total spin $S=2$ (high spin) or $S=0$ (low spin), as sketched in Fig.1 (b). Well above $T_{1/2} \simeq 118$ K, Fe-pic is in the high-spin state (high-temperature high-spin state, HTHS). Upon cooling through $T_{1/2}$, Fe-pic undergoes a crossover to the low-spin state (low-temperature low-spin state, LTLS). The width of the crossover is about 20 K, as observed in the high-spin fraction, $\gamma_{HS}(T)$. The crossover is associated with a ~ 8 % change in the average Fe-N distance. The resulting electron-lattice coupling leads to cooperative interaction among the Fe²⁺ ions,³ as discussed later. In LTLS, a photoexcitation can cause a crossover to a high-spin state. Below 40 K, this photoinduced high-spin state (PIHS) persists even after the excitation is turned off. The half life in γ_{HS} reaches 160 min at 10 K.¹ The development of PIHS involves highly nonlinear responses to the photoexcitation, such as an incubation time, a threshold intensity, a step-like change of γ_{HS} with time, and a domain formation.² These results led to the suggestion that the development of PIHS in Fe-pic should be a transition to a novel macroscopic phase under photoexcitation, referred to as the “*photoinduced phase transition*”.²

To examine this suggestion, it is important to compare the microscopic nature of PIHS with that of HTHS, and to characterize the cooperative interaction among Fe²⁺ ions under photoexcitation. It was found^{5,6,7} that the Raman-infrared selection rules in Fe-pic were modified between HTHS and PIHS, which suggested a photoinduced symmetry lowering in PIHS. In contrast, detailed X-ray diffraction (XRD) study of Fe-pic⁸ found no significant difference in the average crystal structure between HTHS and PIHS. In addition, X-ray absorption fine structure (XAFS) of Fe-pic showed that the local coordinations of the neighboring ions around Fe²⁺ were very similar between HTHS and PIHS.⁹ Recently, a nuclear resonant inelastic scattering (NRIS) experiment was reported on ⁵⁷Fe-enriched Fe-pic.¹⁰ This technique was able to selectively probe the partial vibrational density of states for ⁵⁷Fe. The obtained NRIS spectra were very similar between PIHS and HTHS, showing that the atomic vibration state of Fe²⁺ was also similar.

In this work, we have measured the farinfrared (FIR) absorption spectra of Fe-pic single

crystals in the 80-700 cm^{-1} range. Unlike the previous midinfrared work,⁷ this range can cover the normal-mode vibrations of the FeN_6 cluster. To analyze the observed data, the frequencies of molecular vibrations are calculated for $[\text{Fe}(\text{2-pic})_3]^{2+}$ using density-functional method. Many of the observed absorption lines below 400 cm^{-1} are attributed to the FeN_6 cluster vibrations, which exhibit characteristic intensity changes upon the photo- and temperature-induced spin crossovers. However, they are almost unchanged between HTHS and PIHS. It is concluded that the microscopic vibrational states of the FeN_6 cluster is nearly unchanged between PIHS and HTHS, and that the deformation of 2-pic ligand should play an important role in the development of PIHS.

The single crystals of Fe-pic used in this work were grown by the evaporation method. Plate-shaped samples of approximately $0.7 \times 0.7 \times 0.1 \text{ mm}^3$ were obtained by cleaving the crystals, and mounted on a continuous-flow liquid He cryostat. The FIR absorption experiment was done using a synchrotron radiation (SR) source and a custom-made microscope at the beam line BL43IR, SPring-8.¹¹ The SR source can deliver much higher photon flux density to the sample than the usual FIR sources. Since the Fe-pic single crystals had small sizes and strong FIR absorption, the use of SR was crucial to successfully perform this experiment. A black polyethylene filter was used to cut the visible component of the SR. Photo-excitation of the sample was made using white light from a tungsten lamp. A Si bolometer was used as a detector, and a Fourier-transform interferometer was used to record the spectra. The spectral resolution was set to 4 cm^{-1} .

Figure 2(a) shows the FIR absorption spectra of Fe-pic without photoexcitation at several temperatures across $T_{1/2}$. Here, the absorption is expressed as the optical density (OD), $-\log[I(\nu)/I_0(\nu)]$, where $I(\nu)$ and $I_0(\nu)$ are the transmission spectra with and without the sample, respectively. The detection limit for the weak transmission was about OD=2.8 with an accumulation time of 2 min, and Fig. 2 shows the spectra below OD=2.8 only. The lines above 450 cm^{-1} agree well with those previously observed, which result from the intramolecular vibrations of the 2-pic ligand and ethanol.⁷ In contrast, many of the lines below 450 cm^{-1} are attributed to vibration modes of the FeN_6 cluster, as discussed later. The absorption lines show quite strong intensity variations through $T_{1/2}$. The detailed temperature dependence of several bands and lines, indicated by the labels in Fig. 2, are displayed in Fig. 3. It is seen that the variation of the absorption strength occurs over a width of about 20 K,¹² which agrees well with that of γ_{HS} .⁷ Namely, the absorption strength closely

reflects the evolution of electronic configuration at Fe^{2+} and the associated deformation in the Fe-pic molecule upon the crossover.

Figures 4(a)-(c) present the absorption spectra of Fe-pic in LTLS at 9 K, in PIHS at 9 K, and in HTHS at 140 K, respectively.¹³ Here, spectrum (a) was first recorded, then the sample was photoexcited with a 2 mW/mm² power density of white light for 5 min. After turning off the excitation, spectrum (b) was measured, then the sample was warmed up and spectrum (c) was recorded. The spectra above 450 cm⁻¹ agree well with those reported previously:⁷ The double lines at 530-570 cm⁻¹, marked by the label δ , are observed in PIHS, but not in LTLS and HTHS.^{5,7} In addition, the lines in 570-700 cm⁻¹ range show marked differences between PIHS and HTHS, except for the line *p4* which is due to C-H deformation within the 2-pic ligand.⁷ These lines have been attributed to skeletal vibrations of the aminomethyl group ($-\text{NH}-\text{CH}_2-$) in the 2-pic ligand.⁷ Hence the variations of these lines were regarded as evidence for microscopic deformations in the 2-pic ligand between HTHS and PIHS.

To analyze the data below 450 cm⁻¹, we have calculated the frequencies of infrared-active molecular vibrations for an isolated $[\text{Fe}(\text{2-pic})_3]^{2+}$, using the density-functional method. The calculation was made using the Gaussian '03 program,¹⁴ the details of which were similar to those previously reported.¹⁰ The parameters involved in the calculation were first optimized so as to reproduce the reported molecular structure of $[\text{Fe}(\text{2-pic})_3]^{2+}$, then they were used to calculate the infrared frequencies. The calculated vibration frequencies are displayed by the vertical bars in Figs. 4(a) and (b). It is seen that most of the observed lines have their frequencies close to the calculated ones. (Note that line *e* should be due to ethanol, since it is hardly affected by the crossover.) The lines marked by the asterisks are located far apart from the calculated frequencies. This deviation should be related with the strong hydrogen bonding between the amine group ($-\text{NH}-$) of 2-pic and Cl^- ,⁴ which was neglected in the calculation. The calculated lines below 300 cm⁻¹ in the high-spin states and those below 400 cm⁻¹ in LTLS are mainly derived from the FeN_6 vibration modes. Hence the observed lines in these frequency ranges are also attributed to FeN_6 -based vibrations (except for line *e*). The lines *p1-p3* are attributed to intramolecular vibrations of 2-pic ligand, as in the previous Raman work.^{5,6}

In Fig. 4, the spectra below 300 cm⁻¹ in PIHS and HTHS [(b) and (c)] are very similar to each other. They mainly consist of three strong bands, which are labeled as *c1-c3* in Fig. 4(c). The spectral similarity demonstrates that the microscopic vibrational states of

the FeN_6 cluster are also similar between PIHS and HTHS. In contrast, the spectrum in LTLS, Fig. 4(a), appears quite different from those of the high-spin states. The bands $c1$ - $c3$ are no longer observed in LTLS. Instead, a larger number of narrower lines are observed, which implies a symmetry lowering of FeN_6 in LTLS. The spectral differences should be due to the deformation of FeN_6 and due to changes in the force constants of Fe-N bonds. The occupation of t_{2g} orbitals by 6 electrons in LTLS, as sketched in Fig. 1(b), results in not only the shorter Fe-N distances, but also stronger Fe-N bonds.³ Note that the symmetry of the FeN_6 in the average crystal structure is nearly the same between the high- and low-spin states.^{4,8} Hence, the changes in the force constants seem to have lowered the symmetry of FeN_6 cluster mechanically (not geometrically), resulting in the appearance of a larger number of narrower lines in LTLS.

The present data have demonstrated that the microscopic vibrational states of FeN_6 are very similar between PIHS and HTHS. This is consistent with the previous results of XRD,⁸ XAFS⁹ and NRIS,¹⁰ all of which gave very similar data between PIHS and HTHS. Compared with the previous works, however, it is very important that the present work has explicitly and directly shown the microscopic similarity with a high spectral resolution. In contrast, as already mentioned, the absorption spectrum at 530-700 cm^{-1} range has shown clear differences between PIHS and HTHS, due to skeletal deformation of the 2-pic ligand.^{6,7} Considering these results, therefore, *the most important microscopic difference between the PIHS and HTHS of Fe-pic should be the deformation of 2-pic ligands*. Note that this deformation does not have a long-range order, since the XRD data⁸ show no appreciable deformation of 2-pic in the average crystal structure.

The unusual properties of PIHS, mentioned in the introduction, apparently result from a cooperative interaction (cooperativity) among Fe^{2+} ions. However, a cooperativity is very important also in the thermal spin crossover between HTHS and LTLS.³ This was experimentally demonstrated on the diluted system (Fe, Zn)-pic, where the spin crossover became much broader at low Fe fractions, approaching to that given by the Boltzmann distribution over isolated molecules.¹⁵ An important source of cooperativity is the long-range elastic interaction, caused by the deformation of FeN_6 upon the crossover.^{3,15,16} In this mechanism, an increase in the density of high-spin Fe^{2+} effectively increases the interaction (or equivalently lowers the energy difference between low- and high-spin states¹⁷), accelerating the crossover compared with the isolated case.^{15,17} A theory based on the elastic interaction has

also successfully reproduced two key properties of PIHS under photoexcitation,¹⁷ i.e., the presence of incubation period and the threshold excitation intensity.²

In the above models, however, the microscopic properties involved in the interaction are not taken into account. In addition, short-range interaction among Fe^{2+} ions is neglected. It has been pointed out that the step-like change of γ_{HS} and the phase separation in PIHS cannot be understood without the short-range interaction.¹⁷ It is therefore important to characterize the interaction among Fe^{2+} ions more microscopically. As mentioned before, the -NH- portion of the aminomethyl group in the 2-pic ligand is strongly hydrogen-bonded to the Cl^- anion. This hydrogen bonding is also responsible for the intermolecular bonding and crystallization of Fe-pic molecules.⁴ Hence, the microscopic deformation of 2-pic ligand found in the present work is quite likely to reflect different states of intermolecular bondings between HTHS and PIHS. To further characterize such bonding, it should be very useful to study the vibration modes below the frequency range of this work. The intermolecular vibration modes, which involve the vibration of the entire $[\text{Fe}(\text{2-pic})_3]^{2+}$ ion, are expected to appear well below 80 cm^{-1} . Such modes are expected to be more sensitive to changes in the intermolecular bonding than those observed in this work.

Low-frequency vibrations may be important also in terms of the vibrational entropy.¹⁸ For the thermal crossover in Fe-pic, the phonon part (ΔS_{ph}) of the observed entropy change is as large as 56 %.¹⁹ This acts as a strong driving force for the crossover and also increases the cooperativity.^{3,20} The large ΔS_{ph} results from the strong anharmonicity of the FeN_6 vibrations: When the average lattice constants change upon the crossover, the phonon frequencies also change due to the anharmonicity. Consequently, the phonon density of states is modified, leading to the large ΔS_{ph} .^{18,19} Since the photoinduced crossover is observed at much lower temperatures, high-frequency phonons are quenched, and phonons with much lower frequencies may play important roles in terms of the entropy in PIHS. It is interesting that, in Fig. 4(c), the absorption band *c1* shows significant broadening in HTHS compared in PIHS. This broadening of *c1* seems unusually larger than those of *c2* and *c3*, compared with phonons in the usual solids having similar frequencies. This might be a sign of the strong anharmonicity of the low-frequency FeN_6 vibrations. Again, a further study at lower frequency range is needed to obtain more information about the role of phonon anharmonicity.

In conclusion, we have reported the first FIR absorption study of Fe-pic single crystals in its three characteristic states. The absorption lines below 400 cm^{-1} are mainly attributed

to the FeN_6 vibrations. The spectra are found very similar between PIHS and HTHS, which demonstrate that the microscopic environment at the FeN_6 cluster is also similar. The most important microscopic difference between HTHS and PIHS is the deformation of the 2-pic ligand, which should have important effects on the intermolecular coupling. The present result suggests the importance of further study at lower frequencies, which should give more insight into the microscopic nature of the intermolecular interaction in PIHS.

The experiments at SPring-8 were performed under the approval of JASRI (2004A0480-NSa-np).

* E-mail: okamura@kobe-u.ac.jp

† Present address: SORST, Japan Science and Technology Corporation, Tokyo 113-8656, Japan.

‡ Present address: Department of Chemistry, Carnegie Mellon University, Pittsburgh, Pennsylvania 15213.

- ¹ H. Romstedt, A. Hauser, and H. Spiering, *J. Phys. Chem. Solids*, **59**, 265 (1998).
- ² Y. Ogawa, S. Koshihara, K. Koshino, T. Ogawa, C. Urano, and H. Takagi: *Phys. Rev. Lett.* **84**, 3181 (2000).
- ³ For a review, see for example, P. Gutlich, A. Hauser, and H. Spiering, *Angew. Chem. Int. Ed.* **33** 2024 (1994); P. Gutlich, Y. Garcia, and H.A. Goodwin, *Chem. Soc. Rev.* **29**, 419 (2000).
- ⁴ M. Mikami, M. Konno, and Y. Saito, *Acta. Cryst.* **36**, 275 (1980).
- ⁵ T. Tayagaki and T. Tanaka: *Phys. Rev. Lett.* **86**, 2886 (2001).
- ⁶ T. Tayagaki, K. Tanaka, and H. Okamura, *Phys. Rev. B* **69**, 064104 (2004).
- ⁷ H. Okamura, M. Matsubara, T. Tayagaki, K. Tanaka, Y. Ikemoto, H. Kimura, T. Moriwaki, and T. Nanba, *J. Phys. Soc. Jpn.* **73**, 1355 (2004).
- ⁸ N. Huby, L. Guerin, E. Collet, L. Toupet, J.-C. Ameline, H. Cailleau, T. Roisnel, T. Tayagaki, and K. Tanaka, *Phys. Rev. B* **69**, 020101(R) (2004).
- ⁹ H. Oyanagi, T. Tayagaki, and K. Tanaka, in *X-Ray and Inner-Shell Processes*, ed. A. Marcelli *et al.*, AIP Conf. Proc. **652** (AIP, New York, 2003) p438.
- ¹⁰ G. Juhász, M. Seto, Y. Yoda, S. Hayami, and Y. Maeda, *Chem. Commun.* 2574 (2004).
- ¹¹ Y. Ikemoto, T. Moriwaki, T. Hirono, S. Kimura, K. Shinoda, M. Matsunami, N. Nagai, T. Nanba, K. Kobayashi, and H. Kimura, *Infrared Phys. Tech.* **45**, 369 (2004).

- ¹² The curves in Fig. 3 show the mid-point of the crossover around 103 K, which is lower than $T_{1/2}$. This difference is due to a low thermal contact of the sample with the cryostat, which resulted from our effort of not rigidly mounting the sample to avoid causing an internal strain. At lower temperatures, the thermal conductivity of the sample becomes much higher, and the difference between the measured and actual temperatures should be smaller. Our discussions below will not be affected by such temperature difference.
- ¹³ Due to technical restrictions, the data in Fig. 3 were measured on a different sample from that for the data in Fig. 2. The former was slightly thicker, resulting in the stronger absorption in Fig. 3.
- ¹⁴ M.J. Frisch, *Gaussian '03, Revision B.04* (Gaussian Inc., Pittsburgh, 2003).
- ¹⁵ H. Spiering, E. Meissner, H. Koppen, E.W. Muller, and P. Gutlich, Chem. Phys. **68**, 65 (1982).
- ¹⁶ N. Willenbacher and H. Spiering, J. Phys. C Solid State Phys. **21**, 1423 (1988).
- ¹⁷ K. Koshino and T. Ogawa, J. Phys. Soc. Jpn. **68**, 2164 (1999).
- ¹⁸ A. Bousseksou, J.J. McGarvey, F. Varret, J.A. Real, J.-P. Tuchagues, A.C. Dennis, and M.L. Boillot, Chem. Phys. Lett. **318**, 409 (2000).
- ¹⁹ K. Kaji and M. Sorai, Thermochim. Acta **15**, 185 (1985).
- ²⁰ A. Bousseksou, H. Constant-Machado, and F. Varret, J. Phys. I (France) **5**, 747 (1995).

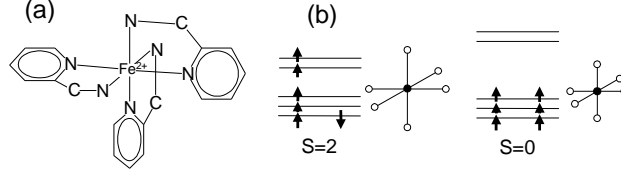


FIG. 1: (a) The structure of $[\text{Fe}(\text{2-pic})_3]^{2+}$. (b) Electron configurations of Fe^{2+} in high-spin ($S=2$) and low-spin ($S=0$) states.

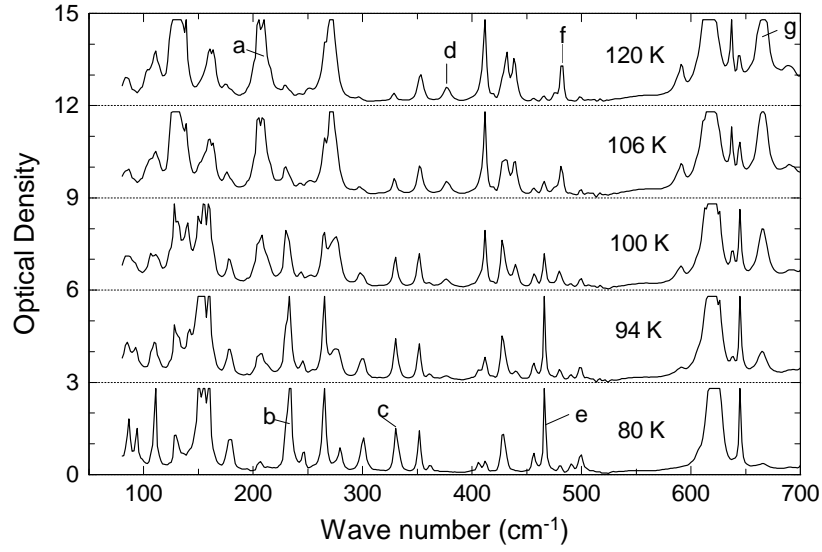


FIG. 2: Optical density of Fe-pic at several temperatures without photo-excitation. The labels a–g indicate the absorption bands and lines analyzed in Fig. 3.

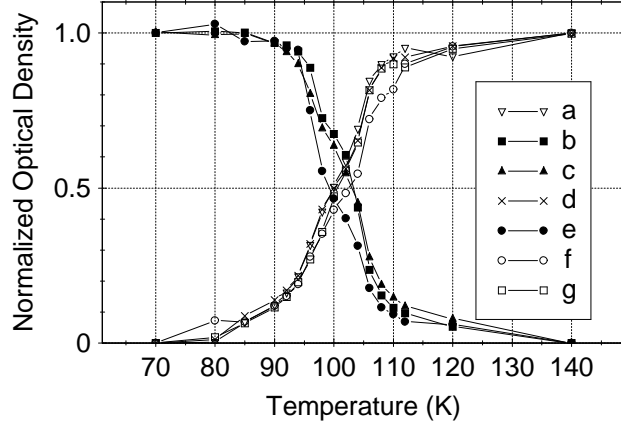


FIG. 3: Optical density (OD) of selected absorption lines and bands for Fe-pic, which are indicated in Fig. 2 by the labels a-f, as a function of temperature. The OD has been integrated over wave number regions of (a) 187-224 cm^{-1} , (b) 224-241 cm^{-1} , (c) 322-340 cm^{-1} , (d) 365-392 cm^{-1} , (e) 462-471 cm^{-1} , (f) 473-488 cm^{-1} , and (g) 650-680 cm^{-1} , then normalized by the difference of OD between 70 and 140 K.

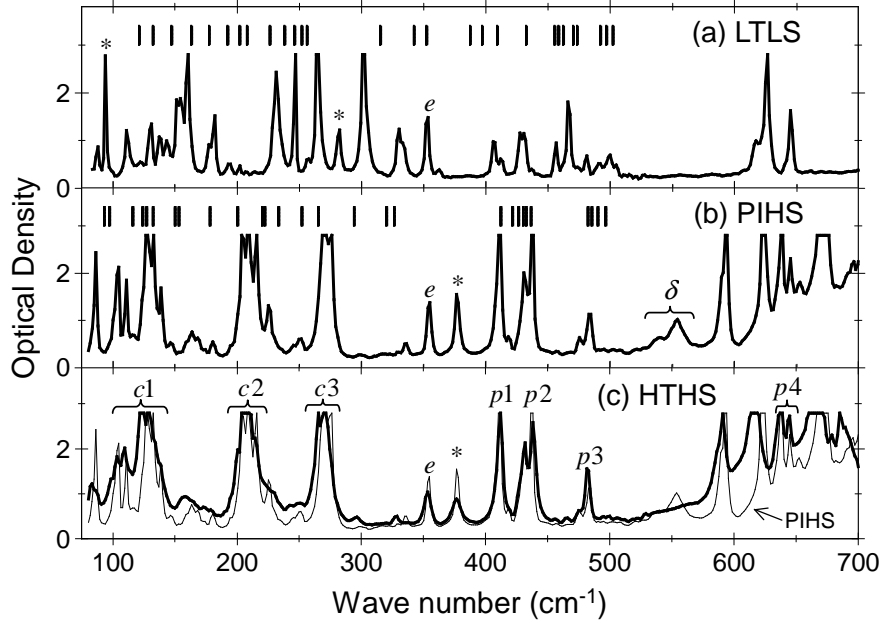


FIG. 4: Optical density spectra of Fe-pic in (a) LTLS at 9 K, (b) PIHS at 9 K, and (c) HTHS at 140 K. The thin curve in (c) is the same as the spectrum in (b), shown for comparison. The vertical bars in (a) and (b) show the calculated frequencies of molecular vibrations for $[\text{Fe}(\text{2-pic})_3]^{2+}$. See text for the labels.